



# Bulk cellulose plastic materials from processing cellulose powder using back pressure-equal channel angular pressing

Xiaoqing Zhang<sup>a,\*</sup>, Xiaolin Wu<sup>b</sup>, Dachao Gao<sup>a</sup>, Kenong Xia<sup>b,\*\*</sup>

<sup>a</sup> CSIRO Materials Science and Engineering, Private Bag 33, Clayton South MDC, Clayton South, VIC 3169, Australia

<sup>b</sup> Department of Mechanical Engineering, The University of Melbourne, VIC 3010, Australia

## ARTICLE INFO

### Article history:

Received 8 August 2011

Received in revised form

27 September 2011

Accepted 7 November 2011

Available online 15 November 2011

### Keywords:

Cellulose

Renewable natural polymers

Crystalline structures

Polymer processing

Equal channel angular pressing

## ABSTRACT

Bulk cellulose plastic materials with a continuous morphology were successfully processed from cellulose powder through back pressure-equal channel angular pressing (BP-ECAP) at 150 °C without using any additives. The strong shear deformation during the process caused an efficient deformation of cellulose granular and crystalline structures, resulting in effective chain penetration and strong intermolecular interactions throughout the whole material. The mechanical behaviour of the cellulose plastics was comparable to those of polymer/cellulose composites. Ball milling the cellulose powder prior to processing disrupted the crystalline structures thus resulting in more significant modifications of the molecular motions of the cellulose. The outcome of this research provides a potential methodology for manufacturing renewable and biodegradable bulk materials from cellulose-based agricultural waste.

© 2011 Elsevier Ltd. All rights reserved.

## 1. Introduction

Cellulose is the most abundant raw polymer in nature and can be considered to be an inexhaustible resource. Its renewable, biodegradable and biocompatible nature in conjunction with low density, good strength and high stiffness, has made it one of the most important natural materials (Klemm, Heublein, Fink, & Bohn, 2005; Ragauskas et al., 2006; Wang & Zhang, 2009, chap. 6). However, thermal processing of natural polymers (not only cellulose, but also starch and plant proteins) using conventional thermal methods is difficult due to strong intra- and intermolecular interactions (hydrogen bonding) and even chemical crosslinking in these materials. Addition of a large amount of plasticizers is necessary for thermal processing starch and proteins to enhance their flexibility and extensibility, and therefore to improve the processing capability. But this method cannot overcome the difficulty in thermal processing cellulose. As a highly crystalline material with a relatively low thermal decomposition temperature, cellulose would normally undergo thermal decomposition before melting upon heating, although melting cellulose under special conditions might be achieved (Nordin, Nyren, & Back, 1973, 1974, Schroeter &

Felix, 2005). Currently cellulose is widely used to blend with other polymers or as a reinforcing agent in the production of polymer composites. In many cases, chemical modification or pretreatment of cellulose is needed in the process (Lu, Zhang, Rong, Shi, & Yang, 2003; Nishino, Matsuda, & Hirao, 2004; Shibata, 2009, chap. 12; Vazquez & Alvarez, 2009, chap. 11; Wang & Zhang, 2009, chap. 6). Development of a new material processing technology for cellulose is desirable for extending the application of cellulose-based materials.

Equal channel angular pressing (ECAP) with back pressure (BP) was originally developed as a novel process to consolidate metal particles (Xia & Wu, 2005; Xia, Wu, Honma, & Ringer, 2007; Wu & Xia, 2007). The oxide layer on the metal surface would be disrupted by the severe shear deformation involved in the process to generate an intimate contact among metal particles. Full density metal was produced with excellent mechanical properties. The other advantage of ECAP consolidation is that the processing can be conducted at temperatures far below the melting temperature of metals. Similar technologies have been applied to polymer materials in the last decade, mainly focused on modification of semi-crystalline polymers and production of their nano-composites (Li, Xia, & Sue, 2000; Phillips, Zhu, & Edward, 2006; Sue & Li, 1998; Sue, Dian, & Li, 1999; Woen & Sue, 2005; Woen, Xia, & Sue, 2005; Xia, Sue, Hsieh, & Huang, 2001; Xia, Sue, & Rieker, 2000). The strong shear deformation during the process (as compared to thermal extrusion in the molten state) could effectively modify polymer morphologies and chain orientation at a temperature below the glass transition

\* Corresponding author. Tel.: +61 3 95452653; fax: +61 3 95441128.

\*\* Corresponding author. Tel.: +61 3 83446664; fax: +61 3 93478784.

E-mail addresses: [Xiaoqing.Zhang@csiro.au](mailto:Xiaoqing.Zhang@csiro.au) (X. Zhang), [K.Xia@unimelb.edu.au](mailto:K.Xia@unimelb.edu.au) (K. Xia).

temperature ( $T_g$ ) for amorphous polymers or the melting temperature ( $T_m$ ) for semi-crystalline polymers, resulting in significant modification of structures and mechanical properties. The advantages of the BP-ECAP technology, especially the low temperature processing capability, are desirable for processing natural polymers into plastic bulk materials. Due to the high shear strain (to 2.0 with a ECAP die of  $90^\circ$ ) achieved in the process (Phillips et al., 2006; Sue & Li, 1998; Sue et al., 1999; Xia et al., 2000), it is expected that the granular structures and crystalline phases of cellulose would be disrupted to some extent and this would be beneficial to the formation of a continuous morphology throughout the material, resulting in the production of cellulose-based biomaterials.

Bulk plastics from raw wheat starch (WS) and wheat gluten (WG) powders were produced by this methodology, and the mechanical strengths of these materials were comparable to those of conventional polymers but stronger than those of thermoplastic WS or plasticized WG (Zhang, Gao, Wu, & Xia, 2008). In the present research, we attempt to use this BP-ECAP methodology to produce bulk plastic materials from cellulose particles which is difficult to be thermally processed by any conventional polymer processing methodologies. A series of advanced material analytical techniques including high-resolution solid-state nuclear magnetic resonance (NMR) and dynamic mechanical analysis (DMA) and X-ray diffraction (XRD) were used to characterize the obtained cellulose plastics. The material morphology, phase structures and molecular motions were examined and correlated to the material performance. The potential in manufacturing bulk cellulose-based natural polymer materials was also discussed.

## 2. Materials and methods

### 2.1. Materials

The cotton linters microcrystalline cellulose powder ( $20\ \mu\text{m}$ ) was purchased from Sigma–Aldrich (product number 310697), and processed without any pre-treatment or additives. Natural moisture content of the cellulose powder was about 6 wt%.

### 2.2. BP-ECAP processing method

The BP-ECAP set-up is shown in Fig. 1, the same as that reported previously (Zhang et al., 2008). The die had a  $90^\circ$  angle with a sharp corner and the channel dimensions were  $9\ \text{mm} \times 9\ \text{mm}$  in cross section. In addition to the forward plunger in the entrance channel, a back plunger was placed in the exit channel to provide a constant BP during ECAP. The die was heated to and kept at a processing temperature using a heating device controlled within  $\pm 1^\circ\text{C}$  with a K-type thermal couple placed close to the sample. The powder was packed in the entrance channel. Once the temperature reached a target value and stabilized, pressing started at a certain speed with a constant back pressure of 100 MPa. The shear strain was 2 for using this  $90^\circ$  die and the stress for pressing the sample through the shear zone varied over a broad range (up to 1200 MPa) for different samples at different processing temperatures.

Ball milling was also conducted in some cases with a ratio of sample/steel balls = 1/20 (in weight) for 2 h (10 min break in the middle of milling to avoid excessive heating) at a speed of 300 rpm using both large and small (1:1 in weight) steel balls (7 and 4 mm in diameter, respectively). ECAP was conducted immediately after the milling following the same procedures.

L-shaped bulk cellulose samples with a cross section of  $\sim 9\ \text{mm} \times 9\ \text{mm}$  and a length of 40–45 mm passing the shear plane (the longer arm of L) were produced by the BP-ECAP method under varied conditions. The sample density was determined by carefully measuring the dimensions and weight. All samples were

conditioned at room temperature ( $20\text{--}22^\circ\text{C}$ ) under relative humidity (RH) of  $50 \pm 2\%$  (achieved by using saturated  $\text{Mg}(\text{NO}_3)_2$  salt solution) for 2 weeks before testing. The moisture contents of the processed samples were around 5–6% after the conditioning, measured as weight loss after heating at  $105^\circ\text{C}$  for 5–6 h to reach a constant weight.

### 2.3. SEM analysis

Fracture surfaces of the samples were produced by bending at specific locations of the ECAP processed sample either before or after passing the shear plane, and examined by scanning electron microscopy (SEM) using Philips FEI XL-30 SFEG. The samples were mounted with double-sided conductive tape and then sputter coated with gold of 20 nm thickness in argon atmosphere. The electron beam with an accelerating voltage of 3–5 kV was used to produce high definition images.

### 2.4. XRD analysis

The X-ray diffraction (XRD) measurements were conducted on a Bruker D8 XRD operating at 40 kV, 40 mA, Cu K $\alpha$  radiation monochromatized with a graphite sample monochromator using program Topas<sup>TM</sup> V4.1. The diffractogram was recorded between  $2\theta$  angles of  $2^\circ$  and  $45^\circ$ .

### 2.5. DMA analysis

A PerkinElmer PYRIS<sup>TM</sup> Diamond DMA was used for DMA experiments in dual cantilever bending mode at a frequency of 1 Hz. The temperature range was set from  $-100$  to  $230^\circ\text{C}$  with a heating rate of  $2^\circ\text{C}/\text{min}$ . The storage modulus ( $E'$ ), loss modulus ( $E''$ ) and  $\tan \delta$  ( $E'/E''$ ) were recorded as a function of temperature throughout the experiment.

### 2.6. NMR spectroscopy

High-resolution solid-state NMR experiments were conducted at room temperature using a Bruker AV500 spectrometer at resonance frequencies of 125 MHz for  $^{13}\text{C}$  and 500 MHz for  $^1\text{H}$ .  $^{13}\text{C}$  NMR spectra were observed under cross polarization (CP), magic angle spinning (MAS) and high power dipolar decoupling (DD) technique. The  $90^\circ$  pulse was  $2.9\ \mu\text{s}$  for  $^1\text{H}$  and  $^{13}\text{C}$ , while the spinning rate of MAS was set at 7.5 kHz. A contact time of 1.0 ms was used for measuring all CP/MAS spectra with a repetition time of 3 s. The  $^{13}\text{C}$  spin-lattice relaxation time ( $T_1$ ) was measured through Torchia pulse sequence (Torchia, 1978). The chemical shift of  $^{13}\text{C}$  spectra was determined by taking the carbonyl carbon of solid glycine (176.3 ppm) as an external reference standard.

## 3. Results and discussion

Bulk cellulose samples were successfully produced by the BP-ECAP method at  $130^\circ\text{C}$  or  $150^\circ\text{C}$ . The density of the proportion after passing the shear plane was  $1.42\text{--}1.52\ \text{g}/\text{cm}^3$ , which is within the range of “true density” of microcrystalline cellulose with 4 wt% of moisture ( $\sim 1.46\ \text{g}/\text{cm}^3$ , Sun, 2005). Fig. 1 shows the changes of the original cellulose powder (Fig. 1A) after being processed by BP-ECAP at  $150^\circ\text{C}$  at a pressing speed of 25 mm/min. Before passing the shear plane, the fracture surface of the sample showed the compression of the packed cellulose particles under high pressure (Fig. 1B), while no such packed particle shapes were observed but a continuous morphology was obtained for the sample after passing the shear plane (Fig. 1C and D). Materials with similar densities were obtained by varying the pressing speed between 0.5 and to 25 mm/min at both 130 and  $150^\circ\text{C}$ . The color of the samples

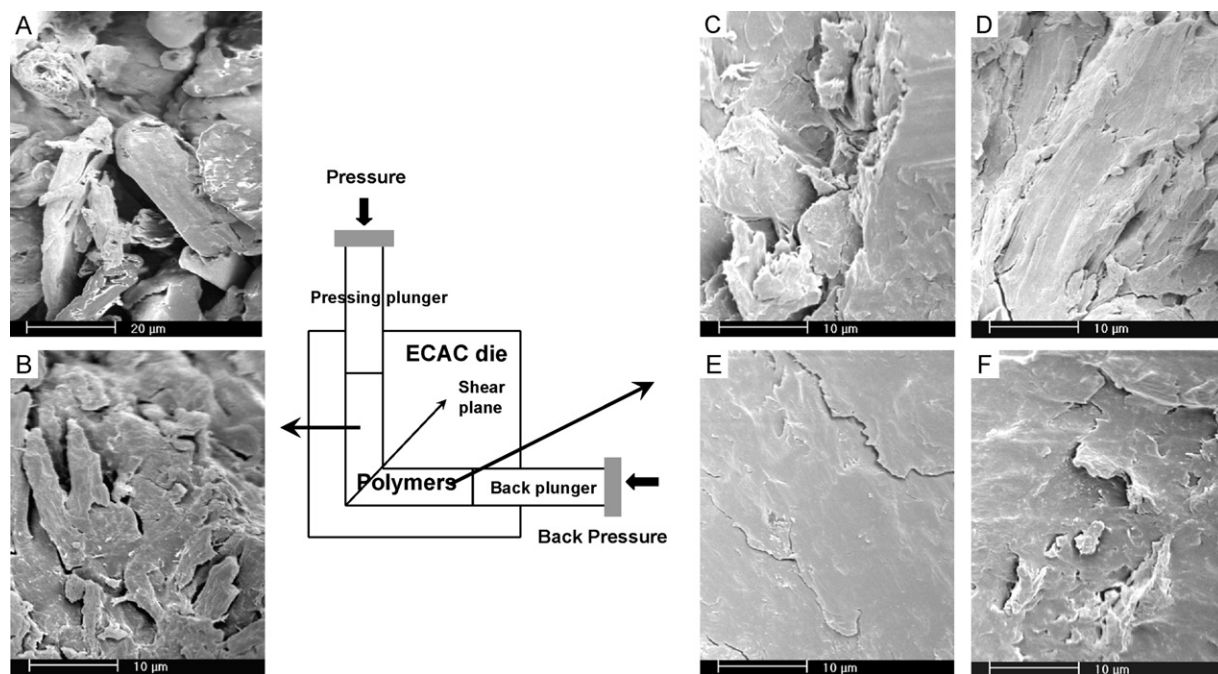


**Fig. 1.** Set-up of BP-ECAP (Zhang et al., 2008) and the SEM image of the cellulose powder (A), fracture surfaces of the cellulose sample before passing the shear plane (B), after passing the shear plane at 150 °C, 25 mm/min without prior-milling (C and D), and with prior-milling (E and F).

turned to dark brown when processing at 200 °C possibly due to a small extend of thermal decomposition, but the sample density remained in the same range as those processed at 130 or 150 °C. Micro-cracking was found parallel to the shear plane of the bulk samples processed especially at lower temperatures (e.g. 130 °C) possibly because the cellulose was not elastic enough to sustain the strong shear deformation at the temperatures.

Ball-milling was also applied to the cellulose particles prior to the ECAP processing in order to disrupt the cellulose particles during the mechanical pre-treatment since such milling had been demonstrated to be effective in reducing crystallinity of cellulose (Paes et al., 2010). Fig. 1E and F shows the fracture surfaces of the cellulose materials obtained at 150 °C at a pressing speed of 25 mm/min after ball-milling. Large smooth morphologies were indeed obtained, suggesting the mobility of some cellulose segments (especially on the surface of cellulose particles) was enhanced due to the milling and then ECAP processing, thus resulting in effective inter-chain penetration and intimate mixing through the whole cellulose materials. Micro-cracking was also reduced and it became possible to conduct mechanical analysis for these bulk cellulose plastic samples.

The DMA curves (storage modulus  $E'$  and  $\tan \delta$  as a function of temperature) of these cellulose samples are shown in Fig. 2 with key data listed in Table 1. Similar to ECAP processed starch or wheat gluten materials (Zhang et al., 2008),  $E'$  of the cellulose samples

**Table 1**  
DMA results of bulk cellulose materials processed by ECAP conditions.<sup>a</sup>

Samples	150 °C, un-milled	200 °C, un-milled	150 °C, milled
$\tan \delta - \beta$ peak (°C)	-42	-27	–
$\tan \delta - \beta$ maximum	0.058	0.042	–
$E'$ at 20 °C (GPa)	1.34	1.06	1.84
$T_{\alpha 1}$ -start (°C)	48	–	47
$T_{\alpha 2}$ -start (°C)	122	190	106
$\tan \delta - \alpha$ peak (°C)	159	–	138
$\tan \delta - \alpha$ maximum	0.100	–	0.181

<sup>a</sup> The ECAP speed was 25 mm/min.

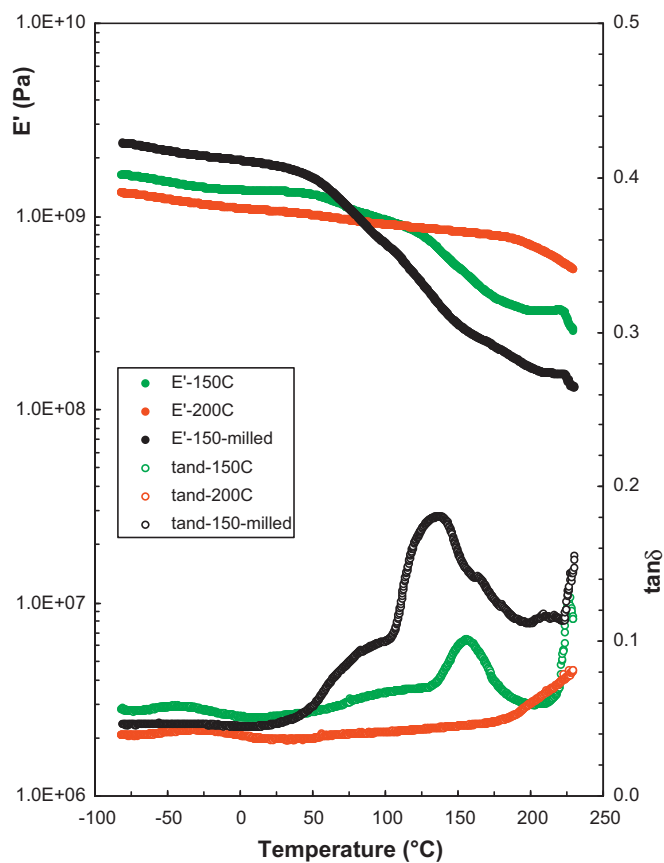


**Fig. 2.** DMA results ( $E'$  and  $\tan \delta$ ) of the bulk cellulose samples processed under different ECAP conditions (pressing speed of 25 mm/min).

experienced a minimal change as temperature increased in the low temperature range, and then dropped at a typical temperature when a glass transition started, while a  $\tan \delta$  peak was observed simultaneously corresponding to the glass transition. For un-milled cellulose processed at 150 °C, a weak  $\beta$ -transition appeared at –42 °C possibly corresponding to the side-chain motions in the material. A weak glass transition started at around 48 °C, as observed by the decreased onset of  $E'$ , accompanied by a very broad  $\tan \delta$  peak. As temperature increased, a strong glass transition started at around 122 °C while a relatively narrow  $\tan \delta$  peak was observed at 159 °C. For the un-milled sample processed at 200 °C, the  $\beta$ -transition became weaker as compared to that processed at 150 °C, and the  $T_g$  shifted to a much higher temperature (190 °C). However, the  $E'$  at room temperature decreased to 1.06 GPa as compared to that processed at 150 °C (1.34 GPa). This result suggests that both thermal crosslinking and decomposition played a role in affecting the material behaviour when conducting the ECAP at 200 °C. The decrease in  $E'$  at room temperature was most likely to be due to a small extent of thermal decomposition while the high  $T_g$  values and weak  $\beta$ -transition should be attributed to the thermal crosslinking effect.

The ball-milled sample ECAP processed at 150 °C displayed much stronger glass transitions (higher  $\tan \delta - \alpha$  maximum) than those of the un-milled samples, and the second glass transition also occurred at a relatively lower temperature, suggesting the decrease in crystallinity due to the prior-milling had resulted in more mobile main-chain motions at  $T_g$  for the amorphous phase in this sample. The  $E'$  at room temperature for the ball-milled sample (1.84 GPa), comparable to those of polymer/cellulose composites (Lu et al., 2003; Shibata, 2009, chap. 12), was also higher than that of the un-milled sample (1.34 GPa). However, the  $\beta$ -transition seemed less pronounced in the ball-milled sample. The results indicate that ball-milling and ECAP processing at 150 °C with a pressing speed of 25 mm/min are promising conditions to produce bulk cellulose plastic materials.

Several typical XRD patterns of the original cellulose powder and bulk cellulose plastics (with no ball-milling before processing) are shown in Fig. 3, displaying cellulose I type diffraction patterns corresponding to (101), (10–1), (002) and (040) crystallographic structures of cellulose (Ishii, Tatsumi, & Matsumoto, 2003; VanderHart & Atalla, 1984; Zhao et al., 2007). The peak intensity in the crystalline diagram of the processed cellulose materials decreased when the samples were processed at higher temperatures (e.g. at 150 and 200 °C) or at higher pressing speeds (e.g. 25 mm/min), indicating a decrease in cellulose's crystallinity under the conditions. Meanwhile, the width of the reflections also became broader especially after processing at a higher temperature or under a higher pressing speed, suggesting that the crystal size or the crystalline regularity of the processed materials was also decreased. The small extent of thermal decomposition at high temperatures (e.g. 200 °C) would also play a role in such a decrease in crystallinity and crystalline regularity.

Ball-milling itself significantly disrupted the crystalline structures as seen in Fig. 4 showing that both crystallinity and crystal size/crystalline regularity were decreased after ball-milling. Note that the BP-ECAP processing thereafter made no much further change in the XRD patterns of the obtained bulk cellulose samples both before passing the shear plane (no ECAP but only be compressed at 150 °C) and after passing the shear plane (Fig. 4). Although the ball-milled cellulose was ECAP processed into bulk material immediately after the milling, the XRD patterns of the ball-milled powder was measured after conditioning and re-crystallization might have occurred during the conditioning period (Paes et al., 2010). Therefore, the decrease in crystallinity due to ball-milling might be slightly underestimated. Because of such a significant decrease in crystallinity and crystalline regularity, we

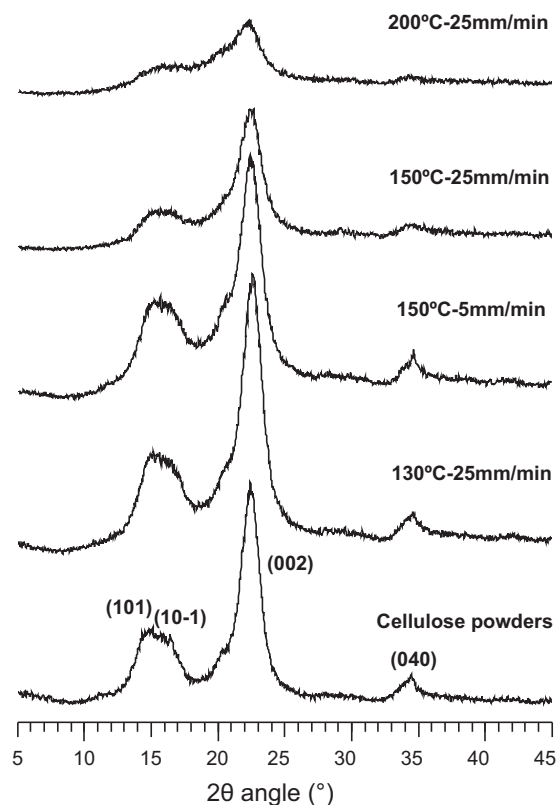


Fig. 3. XRD results of the cellulose powder and the bulk samples processed under different BP-ECAP conditions.

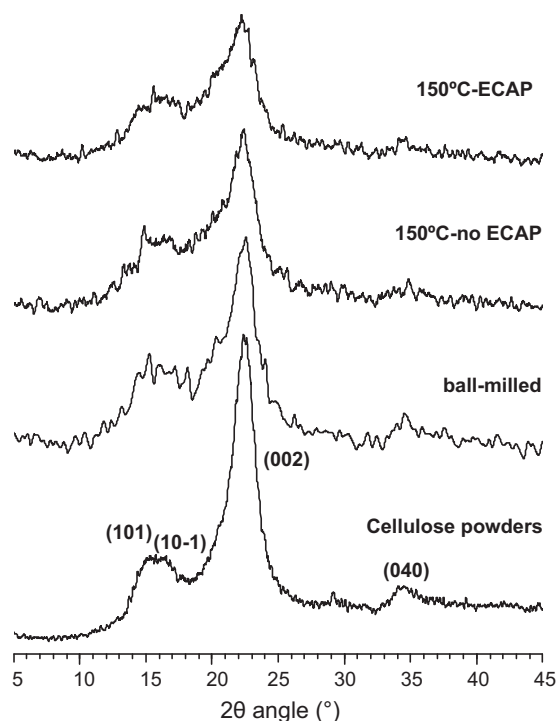
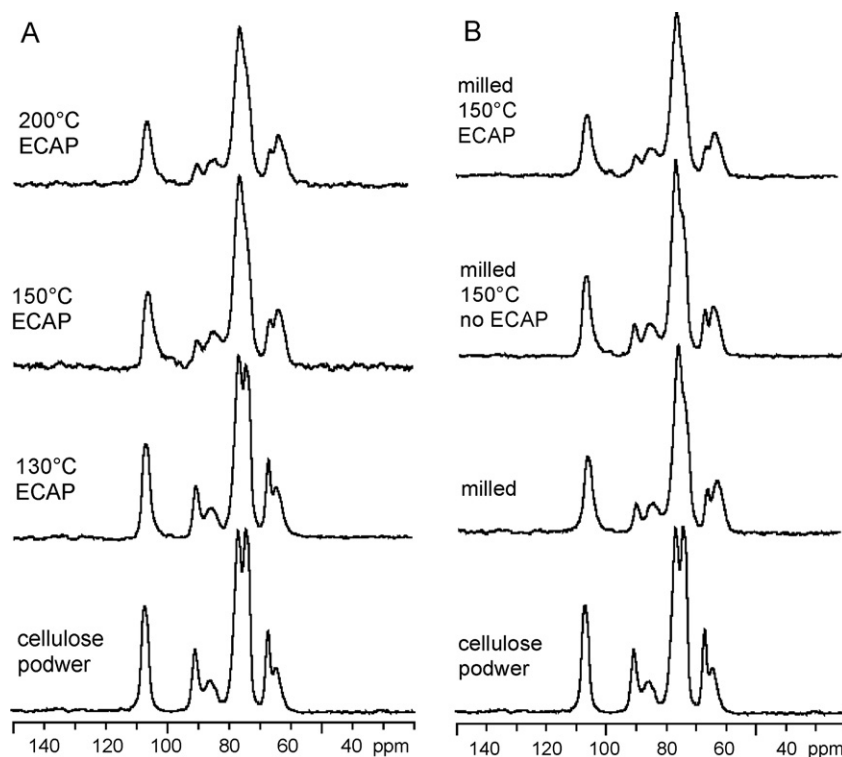


Fig. 4. XRD results of the ball-milled cellulose powder and bulk samples processed under different BP-ECAP conditions (150 °C – no ECAP and – ECAP samples were taken from the same samples processed at 150 °C and 25 mm/min before (no ECAP) and after (ECAP) passing the shear plane).





**Fig. 5.**  $^{13}\text{C}$  CP/MAS NMR spectra of the cellulose samples processed by ECAP at different temperatures without prior-milling (A) and with prior-milling (B). The ECAP speed was 25 mm/min.

did not attempt to conduct a quantitative analysis of the crystal size of these cellulose samples as demonstrated in Newman (1999) and Focher et al. (2001).

High-resolution solid-state NMR is another powerful method to study the change of crystalline structures of cellulose as demonstrated in a series of publications (Atalla & VanderHart, 1999; Horii, Hirai, & Kitamaru, 1987; VanderHart & Atalla, 1984). The  $^{13}\text{C}$  CP/MAS NMR spectrum of the cellulose powder (Fig. 5) displayed the cellulose I poly-morphology as consistent with the XRD results, and the linewidth became broadened after ECAP. The resonances at 106, 80–95, 70–80 and 60–70 ppm are assigned to C-1, C-4, C-2,3,5 and C-6 of the glucose units of cellulose respectively. As reported in the literature (e.g. Newman, 1999), the C-4 signals are particularly well separated with the chemical shift at 91 ppm corresponding to the crystalline phase while that at 85 ppm due to the amorphous phase. Therefore, the spectral deconvolution of the C-4 resonances can be taken as an indicator of crystallinity of the cellulose materials and the data are listed in Table 2. In addition, the two resonances of C-6 at 60–70 ppm also related to the crystalline and amorphous phases of cellulose (although not as separated as

the C-4 resonances), thus the deconvolution results of C-6 peaks are also listed in Table 2 as a comparison with those from C-4.

The crystallinity of the original raw cellulose powder was around 50% which was decreased slightly after BP-ECAP at 130 °C without prior milling. A significant decrease in crystallinity occurred after processing at 150 °C with a pressing speed of 25 mm/min, but further increase in processing temperature (e.g. to 200 °C) did not result in a significant further decrease in crystallinity. The utilization of ball-milling itself had a significant effect on the decrease in the crystallinity of the cellulose powder. The crystallinity of the prior-milled sample ECAP processed at 150 °C was ~25%, quite similar to that processed under the same condition but without prior-milling. It seems the mobile molecular motions at  $T_g$  for the prior-milled sample (DMA data, Fig. 2 and Table 1) could be attributed to the extensive modification of the molecular motions of the amorphous phases during ECAP rather than a further reduction in crystallinity.

For  $^{13}\text{C}$  nuclear systems with very weak spin-diffusion interactions, the spin-lattice ( $T_1$ ) relaxation time (Focher et al., 2001; Torchia, 1978) is sensitive to molecular motions of different groups in different phases. Thus the crystalline and amorphous phases of these bulk cellulose plastics can be examined through  $^{13}\text{C}$   $T_1$  measurements and the data are listed in Table 3. Normally greater  $^{13}\text{C}$   $T_1$  values were obtained for carbon resonances in the crystalline phases while the values for those in the amorphous phases would be much smaller. The intensity changes obtained from deconvolution of the C-4 peaks resulted in single  $^{13}\text{C}$   $T_1$  components at both 91 and 85 ppm, reflecting the nature of the crystalline and amorphous phases respectively. As no deconvolution was applied to the other resonances, two  $^{13}\text{C}$   $T_1$  components were generally obtained for these resonances with the shorter  $T_1$  component corresponding to the amorphous phase while the longer one corresponding to the crystalline phase. However, the ratio of the longer  $^{13}\text{C}$   $T_1$  component cannot be directly taken as the crystallinity especially for the C-1 resonance; as no hydrogen directly was bonded to it,

**Table 2**  
The crystallinity of the cellulose samples measured by NMR.<sup>a</sup>

Cellulose samples	Ratio of peak area at	
	91 ppm/85 ppm	67 ppm/64 ppm
Cellulose powder – 20 $\mu\text{m}$	51/49	50/50
ECAC – 130 °C, 2 mm/min	49/51	46/54
ECAC – 130 °C, 25 mm/min	47/53	45/55
ECAC – 150 °C, 5 mm/min	41/59	42/58
ECAC – 150 °C, 25 mm/min	24/76	32/68
ECAC – 200 °C, 25 mm/min	25/75	27/73
Milled cellulose powder	29/71	32/68
Milled, no ECAC – 150 °C	28/72	33/67
Milled, ECAC – 150 °C, 25 mm/min	24/76	26/74

<sup>a</sup> The resonances at 91 and 67 ppm correspond to the crystalline phase of cellulose.

**Table 3**<sup>13</sup>C T<sub>1</sub> values (s) and the composition of each component (%) of the cellulose samples.<sup>a</sup>

Samples	105 ppm	91 ppm	86 ppm	76 ppm	67 ppm	64 ppm
Cellulose – 20 μm	16.3 ± 3.1 (30%) 142 ± 15 (70%)	235 ± 19	45.0 ± 2.9	15.1 ± 1.8 (42%) 149 ± 17 (58%)	5.9 ± 1.0 (32%) 142 ± 11 (68%)	0.66 ± 0.38 (61%) 8.9 ± 6.2 (39%)
130 °C – ECAP	15.5 ± 3.8 (31%) 114 ± 18 (69%)	141 ± 7	42.4 ± 2.2	14.6 ± 2.8 (45%) 110 ± 14 (55%)	2.8 ± 0.5 (30%) 113 ± 8.9 (70%)	1.01 ± 0.35 (63%) 12.3 ± 6.9 (37%)
150 °C – ECAP	15.3 ± 3.6 (31%) 103 ± 18 (69%)	135 ± 6	44.0 ± 3.0	14.5 ± 3.0 (48%) 87.5 ± 14 (52%)	2.0 ± 0.2 (29%) 78.6 ± 2.9 (71%)	1.05 ± 0.33 (62%) 11.3 ± 7.1 (38%)
200 °C – ECAP	10.1 ± 2.8 (32%) 97.4 ± 17 (68%)	135 ± 4	44.8 ± 1.4	10.6 ± 1.1 (47%) 70.7 ± 6.8 (53%)	2.4 ± 0.6 (32%) 80.2 ± 5.9 (68%)	0.85 ± 0.16 (60%) 8.3 ± 2.2 (40%)
Cellulose-milled	16.1 ± 1.7 (42%) 150 ± 17 (58%)	255 ± 17	42.5 ± 2.0	12.6 ± 1.1 (55%) 106 ± 19 (45%)	3.7 ± 0.6 (34%) 141 ± 19 (66%)	0.90 ± 0.07 (68%) 11.4 ± 1.1 (32%)
Cellulose-milled 150 °C – no ECAP	14.5 ± 1.6 (43%) 133 ± 13 (57%)	189 ± 8	35.9 ± 2.0	12.2 ± 0.9 (58%) 99.4 ± 9 (42%)	2.4 ± 0.4 (34%) 123 ± 9 (66%)	0.85 ± 0.07 (66%) 11.8 ± 2 (33%)
Cellulose-milled 150 °C – ECAP	8.6 ± 2.5 (43%) 70.9 ± 7 (57%)	133 ± 12	31.8 ± 2.8	9.7 ± 1.1 (58%) 58.4 ± 4.4 (42%)	1.9 ± 0.3 (37%) 84.3 ± 7.4 (63%)	0.78 ± 0.06 (68%) 9.3 ± 1.0 (32%)

<sup>a</sup> The ECAP pressing rate of 25 mm/min was used in processing the ECAP samples.

the resonance in different phases might experience different cross-polarization.

Processing the un-milled cellulose at 130 or 150 °C resulted in a decrease in the <sup>13</sup>C T<sub>1</sub> of the C-4 resonance in the crystalline phase but a minimal change was obtained for the C-4 in the amorphous phase. Such a decrease in <sup>13</sup>C T<sub>1</sub> of the crystalline component was obtained for other resonances as well, but the values of the amorphous phase were also decreased for the C-6 resonance, suggesting the modification of the mobility of side-chains. Decreases in <sup>13</sup>C T<sub>1</sub> in the amorphous phases were detected for all carbon resonances when the processing temperature was increased to 200 °C, and these might correspond to thermal crosslinking and/or thermal decomposition which would more likely occur in the amorphous phases. These effects might be responsible for the different XRD patterns of the sample process at 200 °C (Fig. 3).

Ball-milling the cellulose did not change the <sup>13</sup>C T<sub>1</sub> values much for either the crystalline or and amorphous phases, suggesting the milling did not modify the motional nature of the two phases in cellulose although the crystallinity was reduced. For the sample before passing the shear plane (no ECAP), the <sup>13</sup>C T<sub>1</sub> values of both crystalline and amorphous phases were all reduced reflecting the thermal compression effect, and these values were further reduced in the sample when exposed to ECAP deformation (passing the shear plane) at 150 °C. Note that all resonances of the prior-milled sample processed at 150 °C displayed lower <sup>13</sup>C T<sub>1</sub> values as compared to those un-milled samples processed under the same condition, indicating that more extensive motional modification occurred in processing prior-milled cellulose under the BP-ECAP condition, corresponding to its different dynamic mechanical properties.

The outcomes presented in this paper have demonstrated that the BP-ECAP technique is an effective methodology to process cellulose powder into bulk plastic materials which is difficult to achieve by any other conventional polymer thermal processing methods. It seems 150 °C is an optimum processing temperature for cellulose to form a continuous morphology without significant thermal decomposition under the ECAP conditions. This temperature is relatively low as compared to conventional thermal extrusion of semi-crystalline polymers with high melting temperatures, and this is an important advantage for natural polymer processing to overcome their relatively low thermal decomposition temperatures. A fast speed (25 mm/min) during ECAP seemed to be also favorable. The optimum processing conditions will be further investigated including using multi-passes or further increasing the back pressure. Different shear strains may also be tried by varying the channel angles, although the elasticity of the materials needs to be improved to sustain an increased shear deformation. Additives such as plant proteins, hemicellulose, lignin or tannin may

also be used to modify the material elasticity and the mechanical performance of the cellulose materials. Trials on wood particles will also be carried out under an optimum condition to produce bulk “wood plastics” where the existing “impurity” in wood (such as hemicellulose and lignin) might act as useful initial “additives”. The success of this work could lead to a new paradigm for manufacturing plastic materials from agricultural cellulose-based waste and the methodology should be easy to extend into industrial scales.

#### 4. Conclusions

The present study demonstrates that BP-ECAP is an effective method to process cellulose powder into bulk plastic materials without using any additives. The processing temperature could be as low as 150 °C and no significant thermal decomposition of cellulose would occur. Continuous morphologies and reduced crystallinity were obtained for these bulk plastics and their mechanical strength was comparable to those of polymer/cellulose composites. Ball milling the cellulose powder effectively disrupted cellulose structures and decreased the crystallinity, thereby enhanced the chain penetration and intermolecular interactions through the whole materials. Significant modification of the molecular motions was also produced for the cellulose materials under the ECAP condition. The outcome provides a promising opportunity to produce renewable and biodegradable plastics from agricultural cellulose-based waste.

#### Acknowledgements

We thank Ms. Liz Goodall and Mr. Winston Liew at CSIRO for XRD measurements and Mr. Hengky Haryono at the University of Melbourne for assistance with sample preparation.

#### References

- Atalla, R. H., & VanderHart, D. L. (1999). The role of solid state <sup>13</sup>C NMR spectroscopy in studies of the nature of native celluloses. *Solid State Nuclear Magnetic Resonance*, 15, 1–19.
- Focher, B., Palma, M. T., Canetti, M., Torri, G., Cosentino, C., & Gastaldi, G. (2001). Structural differences between non-wood plant celluloses: Evidence from solid state NMR, vibrational spectroscopy and X-ray diffractometry. *Industrial Crops and Products*, 13, 193–208.
- Horii, F., Hirai, A., & Kitamaru, R. (1987). CP/MAS carbon-13 NMR spectra of the crystalline components of native celluloses. *Macromolecules*, 20, 2117–2120.
- Ishii, D., Tatsumi, D., & Matsumoto, T. (2003). Effect of solvent exchange on the solid structure and dissolution behaviour of cellulose. *Biomacromolecules*, 4, 1238–1243.
- Klemm, D., Heublein, B., Fink, H.-P., & Bohn, A. (2005). Cellulose: Fascinating biopolymer and sustainable raw material. *Angewandte Chemie International Edition*, 44, 3358–3393.

- Li, C. K., Xia, Z. Y., & Sue, H. J. (2000). Simple shear plastic deformation behavior of polycarbonate plate: II. Mechanical property characterization. *Polymer*, 41, 6285–6293.
- Lu, X., Zhang, M. Q., Rong, M. Z., Shi, G., & Yang, G. C. (2003). Self-reinforced melt processable composites of sisal. *Composites Science and Technology*, 63, 177–186.
- Newman, R. H. (1999). Estimation of the lateral dimensions of cellulose crystallites using  $^{13}\text{C}$  NMR signal strengths. *Solid State Nuclear Magnetic Resonance*, 15, 21–29.
- Nishino, T., Matsuda, I., & Hirao, K. (2004). All-cellulose composites. *Macromolecules*, 37, 7683–7687.
- Nordin, S., Nyren, J., & Back, E. (1973). Note on molten cellulose produced by a laser beam. *Svensk Papperstidning*, 76, 609–610.
- Nordin, S., Nyren, J., & Back, E. (1974). An indication of molten cellulose produced in a laser beam. *Textile Research Journal*, 44, 152–154.
- Paes, S. S., Sun, S., MacNaughtan, W., Ibbett, R., Ganster, J., Foster, T. J., et al. (2010). The glass transition and crystallization of ball milled cellulose. *Cellulose*, 17, 693–709.
- Phillips, A., Zhu, P. W., & Edward, G. (2006). Simple shear deformation of polypropylene via the equal channel angular extrusion process. *Macromolecules*, 39, 5796–5803.
- Ragauskas, A. J., Williams, C. K., Davison, B. H., Britovsek, G., Cairney, J., & Eckert, C. A. (2006). The path forward for biofuels and biomaterials. *Science*, 311, 484–489.
- Schroeter, J., & Felix, F. (2005). Melting cellulose. *Cellulose*, 12, 159–165.
- Shibata, M. (2009). Poly(lactic acid)/cellulosic fiber composites. In L. Yu (Ed.), *Biodegradable polymer blends and composites from renewable resources* (pp. 287–301). Hoboken, NJ, USA: Wiley, A John Wiley & Sons, Inc.
- Sue, H. J., Dian, H., & Li, C. K. (1999). Simple shear plastic deformation behavior of polycarbonate plate due to the equal channel angular extrusion process. I: Finite element methods modeling. *Polymer Engineering and Science*, 39, 2505–2515.
- Sue, H. J., & Li, C. K. (1998). Control of orientation of lamellar structure in linear low density polyethylene via a novel equal channel angular extrusion process. *Journal of Materials Science Letters*, 17, 853–856.
- Sun, C. Q. (2005). True density of microcrystalline cellulose. *Journal of Pharmaceutical Science*, 94, 2132–2134.
- Torchia, D. A. (1978). The measurement of proton-enhanced carbon- $^{13}\text{C}$   $T_1$  values by a method which suppresses artifacts. *Journal of Magnetic Resonances*, 30, 613–616.
- VanderHart, D. L., & Atalla, R. H. (1984). Studies of microstructure in native cellulose using solid-state  $^{13}\text{C}$  NMR. *Macromolecules*, 17, 1465–1472.
- Vazquez, A., & Alvarez, V. A. (2009). Starch-cellulose fiber composites. In L. Yu (Ed.), *Biodegradable polymer blends and composites from renewable resources* (pp. 241–286). Hoboken, NJ, USA: Wiley, A John Wiley & Sons, Inc.
- Wang, Y., & Zhang, L. (2009). Blends and composites based on cellulose and natural polymers. In L. Yu (Ed.), *Biodegradable polymer blends and composites from renewable resources* (pp. 129–161). Hoboken, NJ, USA: Wiley, A John Wiley & Sons, Inc.
- Woen, J. I., & Sue, H. J. (2005). Effects of clay orientation and aspect ratio on mechanical behavior of nylon-6 nanocomposite. *Polymer*, 46, 6325–6334.
- Woen, J. I., Xia, Z. Y., & Sue, H. J. (2005). Morphological characterization of nylon-6 nanocomposite following a large-scale simple shear process. *Journal of Polymer Science: Part B Polymer Physics*, 43, 3555–3566.
- Wu, X., & Xia, K. (2007). Back pressure equal channel angular consolidation: Application in producing aluminium matrix composites with fine flyash particles. *Journal of Material Processing Technology*, 192–193, 355–359.
- Xia, K., & Wu, X. (2005). Back pressure equal channel angular consolidation of pure Al particles. *Scripta Materialia*, 53, 1225–1229.
- Xia, Z. Y., Sue, H. J., Hsieh, A. J., & Huang, J. W. L. (2001). Dynamic mechanical behavior of oriented semicrystalline polyethylene terephthalate. *Journal of Polymer Science: Part B Polymer Physics*, 39, 1394–1403.
- Xia, Z. Y., Sue, H. J., & Rieker, T. P. (2000). Morphological evolution of poly(ethylene terephthalate) during equal channel angular extrusion process. *Macromolecules*, 33, 8746–8755.
- Xia, K., Wu, X., Honma, T., & Ringer, S. P. (2007). Ultrafine pure aluminium through back pressure equal channel angular consolidation (BP-ECAC) of particles. *Journal of Materials Science*, 42, 1551–1560.
- Zhang, X., Gao, D., Wu, X., & Xia, K. (2008). Bulk plastic materials obtained from processing raw powders of renewable natural polymers via back pressure equal channel angular consolidation (BP-ECAC). *European Polymer Journal*, 44, 780–792.
- Zhao, H., Kwak, J. H., Zhang, C., Brown, H. M., Arey, B. W., & Holladay, J. E. (2007). Studying cellulose fiber structure by SEM, XRD, NMR and acid hydrolysis. *Carbohydrate Polymers*, 68, 235–241.